Heterogeneous and Anomalous Diffusion inside Lipid Tubules

Lin Guo,[†] Pramit Chowdhury,[†] Jiyu Fang,*,[‡] and Feng Gai*,[†]

Department of Chemistry, University of Pennsylvania, Philadelphia, Pennsylvania 19104, and Advanced Materials Processing and Analysis Center, University of Central Florida, Orlando, Florida 32816

Self-assembled lipid tubules with crystalline bilayer walls are promising candidates for controlled drug delivery vehicles on the basis of their ability to release preloaded biological molecules in a sustained manner. While a previous study has shown that the release rate of protein molecules from lipid tubules depends on the associated molecular mass, suggesting that the pertinent diffusion follows the well-known Stokes−Einstein relationship, only a few attempts have been made toward investigating the details of molecular diffusion in the tubule interior. Herein, we have characterized the diffusion rates of several molecules encapsulated in lipid tubules formed by 1,2-bis(10,12-tricosadiynoyl)-*sn*-glycero-3-phosphocholine ($DC_{8,9}PC$) using the techniques of fluorescence recovery after photobleaching (FRAP) and fluorescence correlation spectroscopy (FCS). Our results show that the mobility of these molecules depends not only on their positions in the $DC_{8,9}PC$ tubules but also on their respective concentrations. While the former indicates that the interior of the $DC_{8,9}PC$ tubules is heterogeneous in terms of diffusion, the latter further highlights the possibility of engineering specific conditions for achieving sustained release of a "drug molecule" over a targeted period of time. In addition, our FCS results indicate that the molecular diffusions inside the crystalline bilayer walls of the $DC_{8,9}PC$ tubules strongly deviate from the normal, stochastic processes, with features characterizing not only anomalous subdiffusions but also motions that are superdiffusive in nature.

Introduction

Through organized self-assembly, lipid molecules can form a variety of supramolecular structures with controlled sizes and shapes.[1] Of particular interest are self-assembled hollow lipid tubules with open ends and crystalline walls. It has been shown that a number of synthetic lipids with modified head groups or alkyl chains are able to form tubular structures through rolled-up bilayer sheets in solutions,[2−5] with diameters ranging from 10 nm to 2.0 μm, depending upon the nature of the lipid molecules and conditions under which self-assembly occurs. Unlike carbon nanotubes, which are hydrophobic by nature, lipid tubules with hydrophilic surfaces are ideally suited for providing confined and biologically friendly aqueous environments for various applications.[6−15]

A particularly interesting aspect is the recent suggestion of using lipid tubules as vehicles for delivering drugs in a controlled fashion. For example, long-term release of the transforming growth factor-β from lipid tubules composed of $DC_{8,9}PC$ to cell cultures has been used in soft tissue regenerations.[16,17] In addition, Bellamkonda and co-workers[18] have shown that $DC_{8,9}$-PC tubules embedded in agarose hydrogel release proteins in a sustained manner, a characteristic crucial to controlled drug delivery. Furthermore, and perhaps more importantly, it has been shown that the encapsulated biological molecules inside lipid tubules, such as plasmid DNA[19] and the aforesaid nerve-growth factor,[16,17] maintain their respective native activities. Besides drug delivery, $DC_{8,9}PC$ tubules have also been used in marine applications where the sustained release of antifouling agents preserved the paint coating for an extended period of time.[20]

Though it has been established that encapsulation of various molecules inside lipid tubules results in a sustained release of these entrapped species, not much insight is available with regard to the underlying factors that affect, modify, or control the associated macroscopic release rate. The study of Bellamkonda and co-workers[18] suggests that the release rate of proteins seems to depend on their molecular weight or size, with a relation that larger proteins are released over a longer period of time. While there are no quantitative treatments of this apparent mass dependence, this correlation does seem to suggest that the translational diffusion coefficient of an encapsulated species might play an important role in determining its release rate.

To provide further insights into a tubule's ability to slowly release its payloads, we have studied the diffusion properties of several molecules inside lipid tubules formed by $DC_{8,9}PC$ using the well-known methods of fluorescence recovery after photobleaching (FRAP) and fluorescence correlation spectroscopy (FCS). Both methods, FRAP and FCS, are capable of measuring the characteristic diffusion rate(s) of the molecular species in question. In a typical FRAP experiment, an intense laser light is used to first photobleach fluorophores in a small region of interest (ROI), following which the recovery of the fluorescence, due to the diffusion of unbleached fluorophores into the ROI, is monitored with a highly attenuated laser beam.[21−23] Thus, the FRAP kinetics contain information on the microscopic diffusion constant (and sometimes binding constant) of the fluorescent species in question. On the other hand, the measurement of diffusion using FCS is based on correlating fluorescence intensity fluctuations arising from a fluorescent species diffusing in and out of a small confocal volume.[24] While these methods are complementary to each other, FCS is well suited to monitor diffusions occurring on the submillisecond

---

* To whom correspondence should be addressed. E-mail: gai@sas.upenn.edu (F.G.); jfang@mail.ucf.edu (J.F.).
† University of Pennsylvania.
‡ University of Central Florida.

Diffusion inside Lipid Tubules

J. Phys. Chem. B, Vol. 111, No. 51, 2007 **14245**

time scale, whereas FRAP is more applicable for events taking place on longer time scales (e.g., seconds).[22] In this study, we have investigated the diffusion behaviors of two fluorescent dyes, Rhodamine 6G (R6G) and Nile Red (NR), whose size is comparable to that of many commonly used drugs (e.g., warfarin), as well as that of a 36-residue peptide labeled with tetramethyl rhodamine (hereafter referred to as Z34C-TMR). Our results indicate that the $DC_{8,9}PC$ tubule interior is heterogeneous in terms of molecular diffusion. In addition, the diffusion rate of the aforementioned probe molecules was found to be concentration dependent, a result that has strong implications for "designing" conditions for achieving sustained release of the molecular species of interest in a more effective manner over a desired period of time.

Materials and Methods

R6G (MW = 479), NR (MW = 318), and ANS (MW = 316) were purchased from Molecular Probes (Carlsbad, CA), Sigma (St. Louis, MO), and Acros Organics (Morris Plains, NJ), respectively, and used as received. The peptide (sequence: FNMQCQRRFY-EALHDPNLNE-EQRNAKIKSI-RDDC; MW = 4184) chosen on the basis of its overall high charge density (12 charged amino acid residues) was synthesized using the standard fluoren-9-ylmethoxycarbonyl (Fmoc) based solid-phase method on a PS3 peptide synthesizer (Protein Technologies, MA), purified by reverse-phase chromatography, and verified by matrix-assisted laser desorption ionization (MALDI) mass spectroscopy. TMR-maleimide (Molecular Probes, CA), a thiol reactive dye, was used to label the peptide through the cysteine residue following the protocol available in the Molecular Probes Handbook. Subsequently, the labeled peptide was purified through reverse-phase chromatography and its mass was further verified by MALDI.

Sample Preparation. The lipid tubules were prepared by following the protocol described in detail previously.[25] Briefly, a 5 mg/mL suspension of 1,2-bis(tricosa-10,12-diynoyl)-*sn*-glycero-3-phosphocholine ($DC_{8,9}PC$) (Avanti Polar Lipids, Alabaster, AL) in ethanol/water (70:30 v/v) was cooled from 60 °C to room temperature at a rate of ~0.5 °C/min to yield $DC_{8,9}PC$ tubules with a diameter of ~0.5 μm and a length ranging from 5 to 100 μm.[26] Young's modulus of polymerized $DC_{8,9}PC$ lipid tubules is estimated to be about 1.07 GPa.[27] Prior to each fluorescence experiment, a small number of $DC_{8,9}PC$ lipid tubules was immobilized on a precleaned microscope glass coverslip by drying an aliquot of a PBS buffer solution suspended with lipid tubules overnight in a nitrogen atmosphere. Loading of specific probe molecules (i.e., R6G, NR, or the labeled peptide) was achieved by rehydrating these tubules using a buffer solution containing the desired probe molecules at an appropriate concentration (1 μM for imaging and FRAP experiments and 1 and 10 nM for FCS measurements, respectively). For experiments involving ANS, the tubules were hydrated by buffer containing both ANS (100 nM, 3 μM, or 30 μM) and R6G (1 or 10 nM). The concentration of all stock solutions (in the micromolar range) was determined optically using the respective molar extinction coefficient of the corresponding dye molecules. After incubation of 4 h for equilibration, these tubules were further washed gently with copious quantities of PBS to remove those probe molecules that were nonspecifically adsorbed onto the exterior of the tubules and the coverslip. Subsequent imaging and diffusion experiments were carried out in the presence of PBS buffer to prevent dehydration. Atomic force microscopy showed that the $DC_{8,9}$-PC lipid tubules immobilized on glass slides are stable and retain their cylindrical shapes in aqueous solutions.[25]
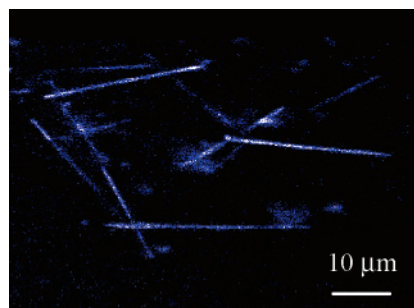

Figure 1. Representative fluorescence confocal image of a group of lipid tubules hydrated with 1 μM R6G.
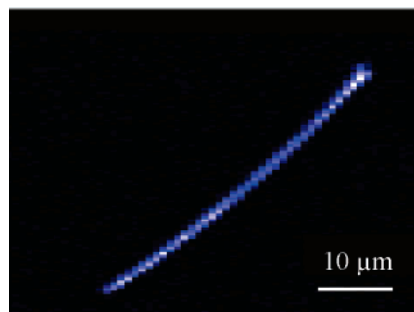

Figure 2. Representative fluorescence confocal image of a lipid tubule hydrated with 1 μM Nile Red. The patterns are due to the large step size used to acquire the current image.

Confocal Microscope. The detail of the confocal fluorescence microscope has been described elsewhere.[28] Briefly, the excitation source at 514.5 nm was derived from the laser lines of an Ar^+ laser (Spectra-Physics, Mt. View, CA), which was brought to a focus in the sample solution by a microscope objective (Nikon 100×, NA 1.3, oil-immersion). The emission was collected by the same objective and was separated from the excitation light by a dichroic mirror. The confocal volume was defined by a 50 μm pinhole. A single interference filter was used to allow only the fluorescence to pass through and reach the detector. Photon counting in real time was achieved by a SPCM-AQR-16 avalanche photodiode (Perkin-Elmer, Canada), and a fast correlator card (Correlator.com, NJ) was used to control the data collection as well as the subsequent autocorrelation analysis for the FCS measurements. Confocal images were acquired by moving the coverslip mounted on a high-resolution piezo-controlled nanopositioning and scanning translation stage (PI, model E501.00). To minimize photobleaching, typically a power of ~350 nW was used in the imaging experiments.

Results and Discussion

Image. Prior to every FRAP experiment, we acquired confocal images of individual tubules to locate their respective positions on the coverslip. As indicated (Figure 1), tubules loaded with R6G are well-resolved, showing the expected shape and size distributions. Similarly, tubules loaded with NR also exhibit strong fluorescence (Figure 2), indicating that such dye molecules can readily partition into the crystalline walls of the $DC_{8,9}PC$ lipid tubule since NR only exhibits detectable fluorescence when sequestered in a nonaqueous or hydrophobic environment.[29] This result is important because it suggests that when interpreting the FRAP and FCS results we have to consider diffusions in at least three broadly defined regions: (1) the aqueous phase in the tubule interior (region-1); (2) the region immediately near the inner surface of the tubule (region-2); (3) the tubule wall (region-3).
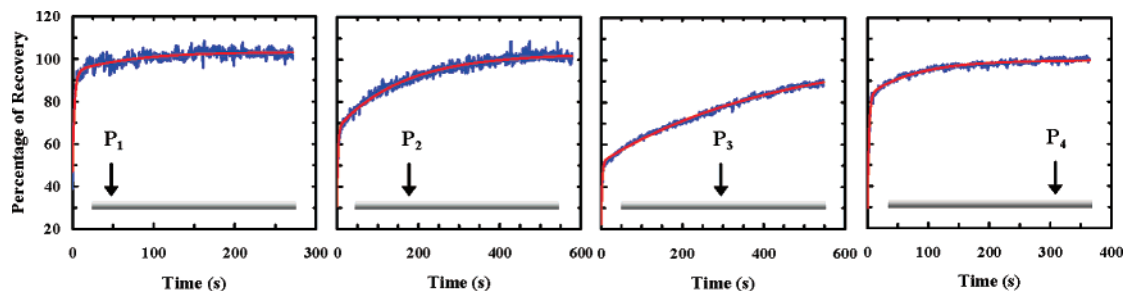
Figure 3. FRAP kinetics of R6G measured at different positions along a lipid tubule, as indicated schematically in the lower portion of each panel. The slow phase was fit to a single-exponential function, and the resultant fitting parameters for different positions are (P$_1$) $A = 0.1$ and $\tau = 67$ s, (P$_2$) $A = 0.34$ and $\tau = 165$ s, (P$_3$) $A = 0.50$ and $\tau = 440$ s, and (P$_4$) $A = 0.16$ and $\tau = 83$ s, where τ is the recovery time constant and A represents the total fractional recovery of the fluorescence signal in this phase.

FRAP Studies. The FRAP measurements were initiated by photobleaching an ROI along a lipid tubule for 30 s with an intense laser beam (about 200 μW before entering the microscope objective), immediately followed by probing the recovery of the fluorescence signal by manually attenuating the photobleaching laser beam to ∼350 nW. The "instrument response" time of the current setup was determined to be about 2.5 s by measuring the FRAP kinetics of R6G in aqueous solution.

As shown in Figure 3, the FRAP traces of R6G obtained at different positions along a tubule indicate that the fluorescence signal recovers in a biphasic manner. The fast phase rises completely within the response time of the instrument and is therefore unresolved in time. In other words, the time resolution of our FRAP setup limits our ability to probe diffusions with an effective diffusion constant smaller than 9×10^{-11} cm^2 s^{-1}, estimated by the method of Axelrod et al.[21] On the other hand, the slow phase is well-resolved and can be well described by a single-exponential function[23] with a time constant of 25 s or greater. Because it has been demonstrated that R6G shows a relatively high affinity toward various membranes,[30] we therefore attribute this phase to diffusions of R6G molecules that are strongly interacting with the lipid molecules of the tubule, either near or inside the walls (i.e., region-2 and region-3, respectively). In support of this assignment, many studies have shown that the diffusion coefficient of dye molecules inside lipid bilayers and/or membranes is smaller than that in aqueous solution at least by 2−4 orders of magnitude,[31] depending on the nature of the lipid domains in question.

Interestingly, we find that the FRAP kinetics of R6G show a distinct position dependence, a feature that has also been observed for diffusions inside silica nanotubes.[32] As shown in Figure 3, on movement from one end of the tubule to the other, the recovery kinetics seem to slow down at the middle while becoming faster at the ends. Repeated measurements show that this trend is maintained for all tubules studied. Typically, at the ends of a tubule the recovery time is ∼70 s, whereas in the middle the recovery time becomes as slow as ∼440 s. While these results suggest that the middle section of the DC$_{8,9}$PC tubule is special in that it more strongly retards the mobility of R6G molecules inside or near its walls, the cause of this retardation is not at all apparent on the basis of our current understanding of the molecular features of the DC$_{8,9}$PC tubule. One possibility is that the lipid packing density reaches a maximum in the central region of the tubule, although other possible interpretations cannot be ruled out.

While the FRAP signal(s) for R6G recovers almost entirely (Figure 3), in contrast, the FRAP data for NR (Figure 4) show that the fluorescence signal only recovers to about 25−45% of its initial value (based upon measurements on different tubules) and mostly within the unresolved fast phase. This indicates that
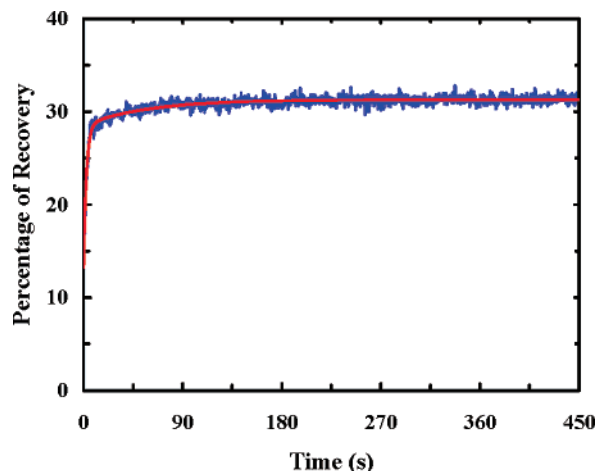

Figure 4. FRAP kinetics of NR measured at the middle region of a lipid tubule. These data indicate that a major portion of the bleached signal does not recover in the observation time window and the recovered portion mostly occurs in the response time of the instrument.

a significant fraction of the fluorophores remains immobile over the observation time window, which is consistent with the fact that NR has a much higher affinity for the membranes than R6G. Taken together, these results provide a phenomenological rationalization of the sustained release of certain molecules encapsulated inside DC$_{8,9}$PC lipid tubules. In other words, these results suggest that the intrinsic hydrophobicity/hydrophilicity of the entrapped species plays an important role in controlling the apparent, macroscopic release rate.

To further examine the effect of various molecular properties (e.g., size or mass and charge) on the rate of diffusion inside lipid tubules, we have also carried out FRAP studies on lipid tubules hydrated with Z34C-TMR. This peptide contains a total of 12 charged residues, and its cross-linked version folds into a helix−turn−helix motif.[33] As shown in Figure 5, the fluorescence signal of Z34C-TMR recovers fully in a single, unresolved phase and is independent of the tubule position probed. Therefore, these results suggest, when compared to those obtained for R6G and NR, that this peptide exhibits very little affinity, if any, toward the interior of the tubule walls. This outcome is consistent with the fact that the sequence of Z34C is rich in charged and polar residues,[33] rendering the peptide a greater preference for the aqueous phase inside the lipid tubules (i.e., region-1). In addition, these results are consistent with the study of Kameta et al.,[15] who demonstrated that electrostatic interactions play a key role in determining the encapsulation efficiency of proteins inside lipid nanotubes.

FCS Studies. Since a significant portion of the FRAP recovery of the aforesaid species occurs within the time resolution of our FRAP setup, we have further probed their
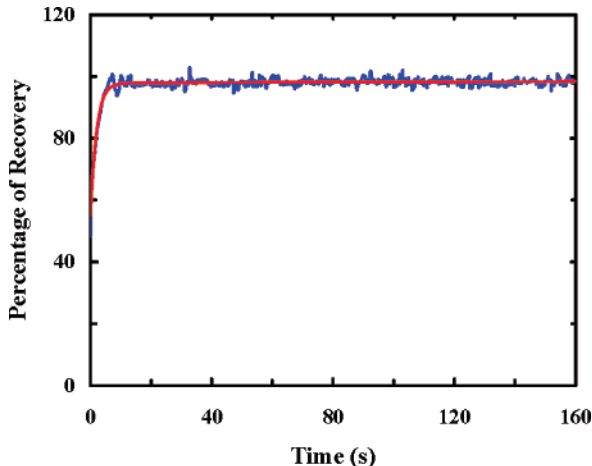
Diffusion inside Lipid Tubules

J. Phys. Chem. B, Vol. 111, No. 51, 2007 **14247**

Figure 5. FRAP kinetics of Z34C-TMR measured at the middle region of a lipid tubule, which indicates that the recovery is too fast to be resolvable by our current FRAP setup.
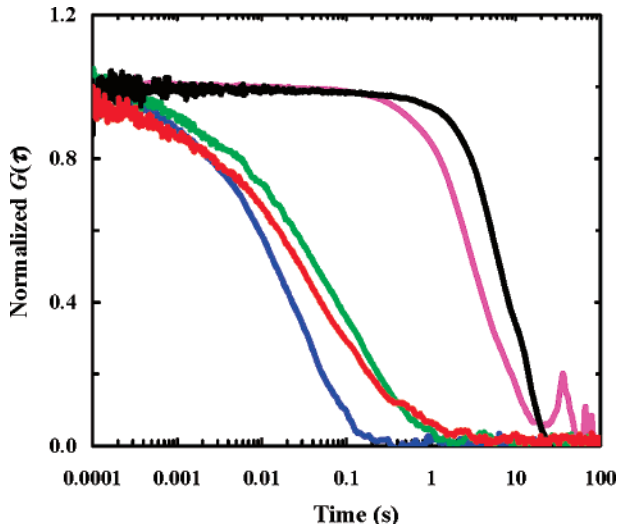

Figure 6. Normalized FCS traces of R6G obtained at the middle region of a lipid tubule and under different conditions: (1) 0.1 nM R6G (magenta); (2) 1 nM R6G (black); (3) 1 nM R6G + 3 μM ANS (blue); (4) 10 nM R6G + 30 μM ANS (green); (5) 10 nM R6G + 100 nM ANS (red). These data can be fit by eq 1 with $n = 2$, and the fitting parameters are listed in Table 1.

characteristic mobilities inside DC$_{8,9}$PC lipid tubules on shorter time scales using FCS. As shown in Figure 6, the autocorrelation traces of R6G, obtained at the middle region of a lipid tubule, show a distinct concentration dependence. Following common practice,[34] the autocorrelation traces, signifying the time for the fluorophore of interest to diffuse across the confocal volume, were further analyzed by using the following equation:

$$G(\tau) = \sum_{i=1}^{n} \frac{1}{N} \left(\frac{1}{1 + \left(\frac{\tau}{\tau_D^i}\right)^{\alpha_i}} \right) \left(\frac{1}{1 + \frac{1}{\omega^2}\left(\frac{\tau}{\tau_D^i}\right)^{\alpha_i}} \right)^{1/2} \quad (1)$$

Here τ_D^i represents the diffusion time constant of the species i and ω refers to the axial to lateral dimension ratio of the confocal volume element. In addition, α_i signifies the extent of deviation from normal diffusion (i.e., when $\alpha = 1$) and N represents the number of fluorescent molecules in the confocal volume. The value of ω for our confocal setup was determined to be 5 by measuring the diffusion of R6G in water, the diffusion coefficient of which is known.[30]

TABLE 1: Characteristic Diffusion Times of R6G at Different Concentrations and with and without the Presence of ANS

[R6G] (nM)	[ANS] (μM)	α_1	τ_D^1	α_2	τ_D^2
0.1	0	1.6	3.6 s	1.0	
1.0	0	1.5	8.4 s	1.0	
10.0	0	0.6	144 ms	1.0	12.6 s
1.0	3	1.4	270 ms	1.0	1.5 ms
10.0	0.1	0.8	416 ms	1.0	450 μs
10.0	30	1.0	1.7 ms	1.0	83 ms

As indicated in Table 1, analyses of the autocorrelation traces presented in Figure 6 reveal that the FCS kinetics obtained at relatively low concentrations (i.e., around 1 nM or lower) can be adequately fit by a single diffusion component. For example, the 1 nM FCS trace of R6G can be well fit by eq 1 with $n = 1$ and $\tau_D = 8.5$ s; however, at higher concentrations (e.g., 10 nM), a two-component diffusion model is required to reliably fit the experimental data. For example, the 10 nM FCS kinetics of R6G are composed of two diffusion components, with time constants of ~144 ms and ~12.5 s, respectively. Taken together, these results indicate that two distinguishable (by the current method) population ensembles, having distinctly different rates of diffusion, coexist. Intuitively, and also on the basis of the FRAP results discussed above, we assign the slower diffusion to those dye molecules moving inside the crystalline walls (i.e., region-3) while the faster one is assigned to those diffusing in the aqueous phase (i.e., region-1).

To further verify these assignments, we have also carried out FCS studies on mixtures of R6G and 1-anilino-8-naphthalene-sulfonate (ANS). ANS is a hydrophobic fluorescent dye and preferentially binds, albeit in a nonspecific manner, to hydrophobic surfaces.[35] Therefore, we expect the ANS molecules to compete with R6G molecules for any potential "binding sites" of the tubule walls, resulting in an increase in the population of the R6G molecules in the aqueous phase compared to those embedded in the bilayer walls of the tubule. Furthermore, ANS has a very small absorption cross section at the current laser excitation wavelength (i.e., 514 nm), thus making negligible contribution to the fluorescence signal. As expected, increasing the concentration of ANS does lead to a considerable decrease in the apparent diffusion time of R6G (Table 1), indicating that the ANS molecules indeed compete favorably for the hydrophobic region of the lipid tubule, driving more R6G molecules into the aqueous phase in the hollow tubule interior. Interestingly, even in the presence of ~30 μM ANS, the τ_D of the fast component is only about 1.7 ms, still significantly larger than the characteristic diffusion time of R6G measured in bulk water (i.e., $\tau_D = 50$ μs for the current setup). This result suggests that the aqueous phase of the tubule interior is far from being bulklike, a feature warranting further exploration in future studies.

In light of the position-dependent FRAP results, we have also carried out similar position-dependent FCS measurements on R6G. As shown in Figure 7, the average diffusion time (i.e., $t_{1/2}$, or the time at which the autocorrelation trace decays to half of its initial value) indeed becomes larger in the middle and smaller at the ends of the tubules. Thus, these FCS measurements, spanning the entire length of the tubule under investigation, further corroborate our FRAP data, indicating that the middle region of the DC$_{8,9}$PC lipid tubules retards diffusion to a greater extent. Finally, it is worth noting that the aforementioned diffusion events revealed by FCS mostly correspond to those giving rise to the unresolved phase in the FRAP experiments as FCS cannot reliably monitor slowly moving molecules due to the effect of photobleaching.
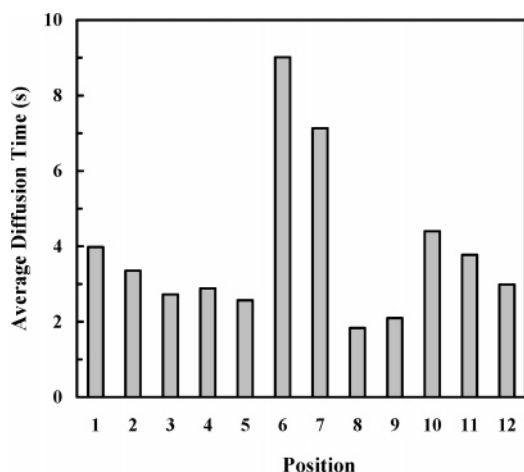
Figure 7. Average diffusion time (i.e., $t_{1/2}$) of R6G versus probing position along a lipid tubule from one end to the other. Positions 6 and 7 correspond to the center region of the tubule, and the distance between two adjacent positions is 2 μm.
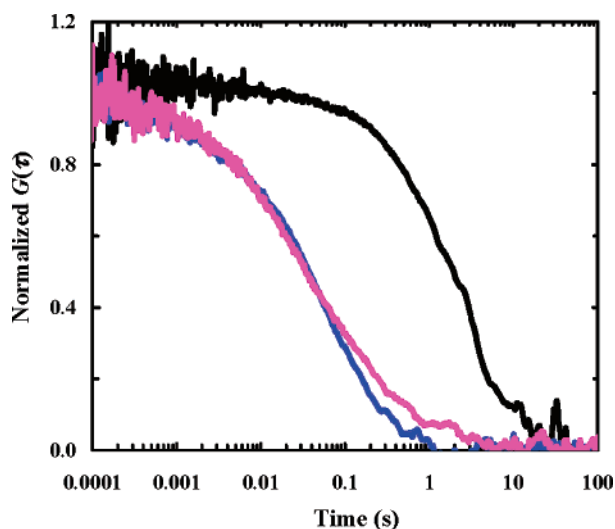

Figure 8. Normalized FCS traces of Z34C-TMR measured at the middle region of a lipid tubule and at different concentrations: (1) 1 nM Z34C-TMR (black); (2) 10 nM Z34C-TMR (blue); (3) 1 nM Z34C-TMR + 3 μM Z34C (magenta). These data can be fit by eq 1 with n = 2, and the fitting parameters are listed in Table 2.

TABLE 2: Characteristic Diffusion Times of Z34C-TMR Measured at Different Conditions

[Z34C-TMR] (nM)	[Z34C] (μM)	α_1	τ_D^1	α_2	τ_D^2
1.0	0	1.0	3.6 s	1.0	1.5 s
10.0	0	0.6	28 ms	1.0	67 ms
1.0	3.0	0.95	300 μs	1.0	50 ms

Interestingly, similar to those observed for R6G, the FCS traces of Z34C-TMR (Figure 8) indicate that the diffusion of this peptide inside the lipid tubule is also composed of two components and depends on concentration (Table 2). For example, at 1 nM its autocorrelation trace can be described by eq 1 with n = 2 with the respective time constants being 1.5 and 3.6 s; however, increasing the concentration of Z34C-TMR to 10 nM leads to a significant reduction in the diffusion times, i.e., to 28 and 67 ms, respectively. This further corroborates our earlier conclusion that Z34C-TMR does not partition inside the tubular walls and hence its interactions with the lipids are limited to the inner surfaces of the tubule walls. Moreover, in the presence of 3 μM unlabeled peptide (i.e., Z34C), wherein the majority of the labeled peptide molecules should sample

the aqueous phase of the tubule interior (i.e., region-1), the recovered diffusion time for the faster component is found to be as low as ~300 μs, a value that is still larger than that of the freely diffusing Z34C-TMR in bulk water (~80 μs). These results are interesting because even in the aqueous phase of the hollow tubule, where the peptide molecules (and also the aforementioned dye molecules) should experience bulklike conditions, the diffusion seems to be hindered. Indeed, it has been shown that, for hollow lipid nanotubes having inner and outer surfaces covered with glucose headgroups, the confined water possesses a higher viscosity and a lower effective polarity than that of bulk water.[36] Thus, the current results provide an apparent reasoning about the sustained release that has been observed for various species encapsulated in $DC_{8,9}PC$ lipid tubules.[16−20]

Anomalous Diffusion. Interestingly, our analyses reveal that most of the FCS traces obtained for R6G and even the peptide at relatively low concentrations (e.g., 1 nM) cannot be fit by the commonly used equation describing the transit of molecules through the confocal volume via normal diffusion (i.e., $\alpha = 1$ in eq 1),[37] namely Fickian diffusion[38] wherein the mean squared displacement $\langle r^2(t)\rangle$ at time t is equal to $6Dt$, where D is the normal, time-independent Stokes−Einstein diffusion constant. Instead, an equation derived to describe anomalous diffusion,[39] i.e.,

$$\langle r^2(t)\rangle = 6\Gamma t^\alpha \qquad (2)$$

has to be used to properly model the R6G FCS curves. In the above equation, the value of the exponent α denotes the extent of deviation from normal diffusion ($\alpha = 1$). For $\alpha < 1$, the process is known as subdiffusion, whereas, for $\alpha > 1$, the underlying process is considered to be in the superdiffusive regime. Anomalous diffusions have been observed in membranes, where a number of interactions can hinder the molecular motions of interest.[40] In addition, it has been shown that the diffusion of enzymes in certain nanotube-vesicle networks can also become anomalous.[12]

For R6G at low concentrations, the value of α was found to be in the range 1.3−2, indicating that the pertinent diffusion inside the tubule walls (i.e., region-3) is superdiffusive in nature. To further verify this observation, we have carried out FCS studies on NR since it has a much larger affinity toward membranes than R6G and hence should be a more reliable probe of anomalous diffusion inside the crystalline tubular walls. As shown in Figure 9, the FCS trace of NR, probed at the middle region of a $DC_{8,9}PC$ tubule, cannot be described either by a simple normal diffusion only model ($\alpha = 1$) or by an anomalous diffusion only model but is reliably fitted by eq 1 that encompasses both the aforesaid features. To our surprise, repeated measurements indicate that the value of α in most cases is greater than 1 (i.e., 1.2−2.0), thus further corroborating the superdiffusive nature of small molecules inside the lipid region (or region-3) of the $DC_{8,9}PC$ tubule.

In comparison, almost all the previous studies regarding anomalous diffusion in membranes have reported an α of less than 1, typically in the range 0.2−0.9,[41−43] manifesting various interactions that retard the motion of the probe molecule. In this regard, the observation of the phenomenon of superdiffusion in lipid tubules is indeed surprising. While the possibility of such a motion existing in cellular structures or synthetic lipids has been hinted at previously[44] and it has been shown that a chaotic Hamiltonian system might give rise to turbulent diffusions with $\alpha = 3$,[45] not much evidence to this end exists for membrane systems to date. In the case of the lipid tubules, such

Diffusion inside Lipid Tubules

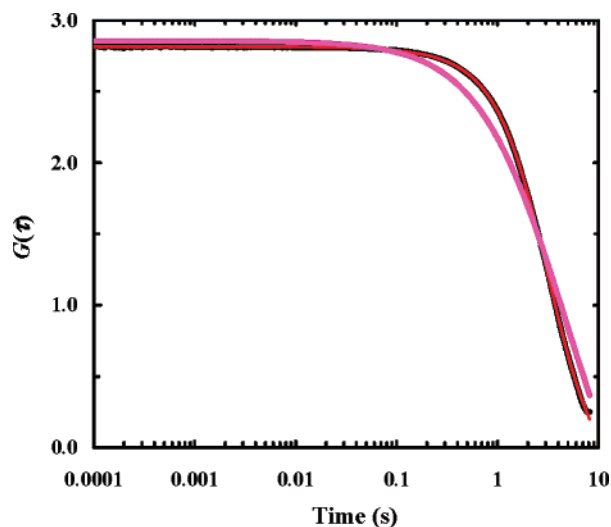*J. Phys. Chem. B, Vol. 111, No. 51, 2007* **14249**

Figure 9. Representative FCS trace (black) of NR (1 nM) measured at the middle of a lipid tubule. The line in red corresponds to a fit to eq 1 with $n = 2$ and the parameters $\alpha_1 = 1.8$, $\tau_D^1 = 3.2$ s, $\alpha_2 = 1.0$, and $\tau_D^2 = 2.2$ s. Also shown in magenta is a fit to eq 1 with two normal diffusion components.

superdiffusive motions might be due to the well-ordered and crystalline-like packing of the lipid molecules,[46−48] forcing the dye molecules to diffuse along a certain well-defined direction, akin to that observed along the flow in a microcapillary.[49] Indeed, it has been proposed that diffusion in multilamellar systems is anisotropic and that the motion of those molecules confined to the lipid matrix is largely restricted along the plane of the bilayer.[50]

Conclusions

In summary, we present here a detailed study of diffusion inside $DC_{8,9}PC$ lipid tubules using the methods of FRAP and FCS. Our results reveal that the tubule interior is very heterogeneous in terms of diffusion. Both FRAP and FCS data indicate that the diffusion becomes slower in the middle and faster at the ends of the tubules. Furthermore, our results show that the diffusion is concentration dependent, with the relation that a faster diffusion rate correlates with a higher concentration. This result might prove to be very useful for designing conditions for the "controlled and sustained" release of "a drug molecule" from $DC_{8,9}PC$ lipid tubules. Moreover, our FCS results reveal that the diffusion inside the lipid tubule walls is superdiffusive in nature, suggesting that the well-ordered packing of lipid molecules in the lipid tubule may provide a special environment for directed diffusion.

References and Notes

(1) Collier, J. H.; Messersmith, P. B. *Annu. Rev. Mater. Res.* **2001**, *31*, 237.

(2) Spector, M. S.; Selinger, J. V.; Schnur, J. M. *Materials-Chirality: Vol. 24 of Topics in Stereochemistry: Chiral Molecular Self-Assembly*; Green, M. M., Nolte, J. M., Meijer, E. W., Eds.; Wiley: Hoboken, NJ, 2003.

(3) Shimizu, T.; Masuda, M.; Minamikawa, H. *Chem. Rev.* **2005**, *105*, 1401.

(4) Brizard, A.; Oda, R.; Huc, I. *Top. Curr. Chem.* **2005**, *256*, 167.

(5) Fang, J. Y. *J. Mater. Chem.* **2007**, *17*, 3479.

(6) Letellier, D.; Sandre, O.; Menager, C.; Cabuil, V.; Lavergne, M. *Mater. Sci. Eng., C* **1997**, *5*, 153.

(7) Lvov, Y. M.; Price, R. R.; Selinger, J. V.; Singh, A.; Spector, M. S.; Schnur, J. M. *Langmuir* **2000**, *16*, 5932.

(8) Yang, B.; Kamiya, S.; Yoshida, K.; Shimizu, Y.; Koshizaki, N.; Shimizu, T. *Chem. Mater.* **2004**, *16*, 2826.

(9) Kameta, N.; Masuda, M.; Minamikawa, H.; Goutev, N. V.; Rim, J. A.; Jung, J. H.; Shimizu, T. *Adv. Mater.* **2005**, *17*, 2732.

(10) Yu, L.; Banerjee, I. A.; Gao, X.; Nuraje, N.; Matsui, H. *Bioconjugate Chem.* **2005**, *16*, 1484.

(11) Zhao, Y.; Mahajan, N.; Fang, J. Y. *Small* **2006**, *2*, 364.

(12) Sott, K.; Lobovkina, T.; Lizana, L.; Tokarz, M.; Bauer, B.; Konkoli, Z.; Orwar, O. *Nano Lett.* **2006**, *6*, 209.

(13) Karlsson, R.; Karlsson, M.; Karlsson, A.; Cans, A.-S.; Bergenholtz, J.; Akerman, B.; Ewing, A. G.; Voinova, M.; Orwar, O. *Langmuir* **2002**, *18*, 4186.

(14) Brenner, H.; Gaydos, L. J. *J. Colloid Interface Sci.* **1977**, *58*, 312.

(15) Kameta, N.; Masuda, M.; Minamikawa, H.; Mishima, Y.; Yamashita, I.; Shimizu, T. *Chem. Mater.* **2007**, *19*, 3553.

(16) Schnur, J. M.; Price, R. R.; Rudolph, A. S. *J. Controlled Release* **1994**, *28*, 3.

(17) Spargo, B. J.; Cliff, R. O.; Rollwage, F. M.; Rudolph, A. S. *J. Microencapsulation* **1995**, *12*, 247.

(18) Meilander, N. J.; Yu, X.; Ziats, N. P.; Bellamkonda, R. V. *J. Controlled Release* **2001**, *71*, 141.

(19) Meilander, N. J.; Pasumarthy, M. K.; Kowalczyk, T. H.; Cooper, M. J.; Bellamkonda, R. V. *J. Controlled Release* **2003**, *88*, 321.

(20) Price, R.; Schnur, J. M. *J. Coat. Technol.* **2003**, *75*, 53.

(21) Axelrod, D.; Koppel, D. E.; Schlessinger, J.; Elson, E.; Webb, W. W. *Biophys. J.* **1976**, *16*, 1055.

(22) Sprague, B. L.; McNally, J. G. *Trends Cell Biol.* **2005**, *15*, 84.

(23) Sprague, B. L.; Pego, R. L.; Stavreva, D. A.; McNally, J. G. *Biophys. J.* **2004**, *86*, 3473.

(24) Rigler, R.; Mets, Ü.; Widengren, W.; Kask, P. *Eur. Biophys. J.* **1993**, *22*, 169.

(25) Mahajan, N.; Fang, J. Y. *Langmuir* **2005**, *21*, 3153.

(26) Yager, P.; Schoen, P. E. *Mol. Cryst. Liq. Cryst.* **1984**, *106*, 371.

(27) Zhao, Y.; An, L.; Fang, J. Y. *Nano Lett.* **2007**, *7*, 1360.

(28) Purkayastha, P.; Klemke, J. W.; Lavender, S.; Martinez, R. O.; Cooperman, B. S.; Gai, F. *Biochemistry* **2005**, *44*, 2642.

(29) Greenspan, P.; Fowler, S. D. *J. Lipid Res.* **1985**, *26*, 781.

(30) Pramanik, A.; Thyberg, P.; Rigler, R. *Chem. Phys. Lipids* **2000**, *104*, 35.

(31) Korlach, J.; Schwille, P.; Webb, W. W.; Feigenson, G. W. *Proc. Natl. Acad. Sci. U.S.A.* **1999**, *96*, 8461.

(32) Okamoto, K.; Shook, C. J.; Bivona, L.; Lee, S. B.; English, D. S. *Nano Lett.* **2004**, *4*, 233.

(33) Du, D. G.; Gai, F. *Biochemistry* **2006**, *45*, 13131.

(34) Banks, D. S.; Fradin, C. *Biophys. J.* **2005**, *89*, 2960.

(35) Pastukhov, A. V.; Ropson, I. J. *Proteins* **2003**, *53*, 607.

(36) Guo, Y. L.; Yui, H.; Minamikawa, H.; Masuda, M.; Kamiya, S.; Sawada, T.; Ito, K.; Shimizu, T. *Langmuir* **2005**, *21*, 4610.

(37) The effective value of ω could be smaller than 5 due to the fact that the diameter of the lipid tubule is smaller than the axial spread of the excitation beam. However, using a different ω value (e.g., 0.5−5) in eq 1 for $\alpha = 1$ does not improve the quality of the fit.

(38) Gorenflo, R.; Mainardi, F.; Moretti, D.; Pagnini, G.; Paradisi, P. *Chem. Phys.* **2002**, *284*, 521.

(39) Saxton, M. J. *Biophys. J.* **2001**, *81*, 2226.

(40) Saxton, M. J.; Jacobson, K. *Annu. Rev. Biophys. Biomol. Struct.* **1997**, *26*, 373.

(41) Ghosh, R. N.; Webb, W. W. *Biophys. J.* **1994**, *66*, 1301.

(42) Feder, T. J.; Brust-Mascher, I.; Slattery, J. P.; Baird, B.; Webb, W. W. *Biophys. J.* **1996**, *70*, 2767.

(43) Schwille, P.; Haupts, U.; Maiti, S.; Webb, W. W. *Biophys. J.* **1999**, *77*, 2251.

(44) Saxton, M. J. *Biophys. J.* **1993**, *64*, 1766.

(45) Shlesinger, M. F.; Zaslavsky, G. M.; Klafter, J. *Nature* **1993**, *363*, 31.

(46) Thomas, B. N.; Safinya, C. R.; Plano, R. J.; Clark, N. A. *Science* **1995**, *267*, 1635.

(47) Rudolph, A. S.; Singh, B. P.; Singh, A.; Burke, T. G. *Biochim. Biophys. Acta* **1988**, *943*, 454.

(48) Lando, J. B.; Sudiwala, R. V. *Chem. Mater.* **1990**, *2*, 594.

(49) Lenne, P.-F.; Colombo, D.; Giovannini, H.; Regnault, H. *Single Mol.* **2002**, *4*, 194.

(50) Gaede, H. C.; Gawrisch, K. *Biophys. J.* **2003**, *85*, 1734.